Anti-inflammatory activity of essential oils from Tunisian aromatic and medicinal plants and their major constituents in THP-1 macrophages

Renato B Pereira, Fatma Zohra Rahali, Ralph Nehme, Hanen Falleh, Mariem
Ben Jemaa, Ibtissem Hamrouni Sellami, Riadh Ksouri, Said Bouhallab,
Fabrizio Ceciliani, Latifa Abdennebi-Najar, et al.

Anti-inflammatory activity of essential oils from Tunisian aromatic and medicinal plants and their major constituents in THP-1 macrophages

Renato B. Pereira [a,*], Fatma Zohra Rahali [b], Ralph Nehme [c], Hanen Falleh [b], Mariem Ben Jemaa [b], Ibtissem Hamrouni Sellami [b], Riadh Ksouri [b], Said Bouhallab [d], Fabrizio Ceciliani [e], Latifa Abdennebi-Najar [c,f], David M. Pereira [a,*]

[a] REQUIMTE/LAQV, Laboratório de Farmacognosia, Departamento de Química, Faculdade de Farmácia, Universidade do Porto, R. Jorge Viterbo Ferreira, n° 228, 4050-313 Porto, Portugal
[b] Laboratory of Aromatic and Medicinal Plants, Biotechnology Center of Borj-Cédria, BP 901 2050 Hammam-Lif, Tunisia
[c] Quality and Health Department, IDELE Institute, 149 rue de Bercy, 75595 Paris Cedex 12, France
[d] INRAE, Institut Agro, STLO, F-35042 Rennes, France
[e] Department of Veterinary Medicine, Università degli Studi di Milano, 20122 Milano, Italy
[f] Centre de Recherche Saint-Antoine (CRSA), Sorbonne University, INSERM UMR_S_938, 75020 Paris, France

ABSTRACT

In this study, the capacity of eight essential oils (EOs), sage (*Salvia officinalis*), coriander (*Coriandrum sativum*), rosemary (*Rosmarinus officinalis*), black cumin (*Nigella sativa*), prickly juniper (*Juniperus oxycedrus*), geranium (*Pelargonium graveolens*), oregano (*Origanum vulgare*) and wormwood (*Artemisia herba-alba*), on the inhibition of NF-κB activation was screened at concentrations up to 0.25 μL/mL using THP-1 human macrophages bearing a NF-κB reporter. This screening selected coriander, geranium, and wormwood EOs as the most active, which later evidenced the ability to decrease over 50 % IL-6, IL-1β, TNF-α and COX-2 mRNA expression in LPS-stimulated THP-1 macrophages. The chemical composition of selected EOs was performed by gas chromatography–mass spectrometry (GC–MS). The two major constituents (>50 % of each EO) were tested at the same concentrations presented in each EO. It was demonstrated that the major compound or the binary mixtures of the two major compounds could explain the anti-inflammatory effects reported for the crude EOs. Additionally, the selected EOs also inhibit >50 % caspase-1 activity. However, this effect could not be attributed to the major components (except for β-citronellol/geranium oil, 40 %/65 % caspase-1 inhibition), suggesting, in addition to potential synergistic effects, the presence of minor compounds with caspase-1 inhibitory activity.

These results demonstrated the potential use of the EOs obtained from Tunisian flora as valuable sources of anti-inflammatory agents providing beneficial health effects by reducing the levels of inflammatory mediators involved in the genesis of several diseases.

1. Introduction

Inflammation is regarded as an important physiological reaction responsible for manifestations of various chronic diseases, including autoimmune diseases such as arthritis and diabetes, Alzheimer's disease and cancer (Chen et al., 2018; Furman et al., 2019). Inflammatory diseases are generally treated with steroidal and non-steroidal anti-inflammatory drugs, their long-term use causing various side effects, reducing their use in specific segments of the population (Ho, Li, Weng, Hua, & Ju, 2020; Pérez, Zavala, Arias, & Ramos, 2011; Vonkeman & van de Laar, 2010). Hence, natural, safe, and efficient plant-based anti-inflammatory ingredients with minimal side effects are required.

Many medicinal and aromatic plants have long been known in ethnomedicine to prevent and treat different human diseases (Pérez et al., 2011). Their application is often related to essential oils (EOs) possessing remarkable anti-inflammatory, antitumor, antioxidant and antimicrobial properties desirable in the food, cosmetic, agricultural and pharmaceutical industries (Falleh, Ben Jemaa, Saada, & Ksouri, 2020; Miguel, 2010a). EOs have a complex composition, containing from a dozen to several hundred components, many of which are terpenes with

low molecular weight (Spisni et al., 2020). The proportions of these constituents in EOs vary greatly, however, major components can constitute up to 85 % of the oil, while the remaining components can be present in trace amounts (Miguel, 2010b). This plethora of molecules can target multiple inflammatory signaling pathways, making the identification of a leading anti-inflammatory molecule in EOs and elucidation of the exact mechanism of action an herculean task (Nehme et al., 2021). Therefore, exploring the anti-inflammatory effects and underlying mechanisms of EOs, as well as their active components, will aid in understanding the use of aromatic plants as anti-inflammatory drugs for the treatment of inflammation.

Herein, we reported the *in vitro* anti-inflammatory activity of eight EOs obtained by hydrodistillation of different aromatic and medicinal plants collected in Tunisia in the frame of a EU-PRIMA project for exploitation of potential bioactive molecules using this country's biodiversity. Many of the species studied are widely used in several Mediterranean countries in cookery, thus justifying their interest to the field of food research. Among them, the three most promising, *Coriandrum sativum* (coriander), *Pelargonium graveolens* (geranium) and *Artemisia herba-alba* (wormwood), were chemically characterized by GC–MS and explored, *in vitro*, for their anti-inflammatory properties. With this aim in view, the major constituents were also screened to determine, from a mechanistic point of view, which is responsible for the observed anti-inflammatory effects in THP-1 macrophages.

2. Materials and methods

2.1. Reagents and Standards

Lipopolysaccharide (LPS) O127:B8 from *Escherichia coli*, 3-(4,5-dimethylthiazol-2-yl)-2,5-diphenyltetrazolium bromide (MTT) (Product No. M2128), dimethyl sulfoxide (DMSO) (Product No. D2650), HEPES 1 M, triton X-100, trypan blue, propan-2-ol, dexamethasone, linalool, α-pinene, β-citronellol, geraniol, α-thujone and camphor were from Sigma-Aldrich (St. Louis, USA). Dulbecco's Modified Eagle Medium (DMEM), Roswell Park Memorial Institute (RPMI) 1640, fetal bovine serum (FBS), Hank's balanced salt solution (HBSS), 0.25 % trypsin-EDTA (1X) and penicillin–streptomycin solution (penicillin 10,000 units/mL and streptomycin 10000 μg/mL) were purchased from GIBCO, Invitrogen (Grand Island, USA). Caspase-Glo® 1 inflammasome assay kit was from Promega Corporation. COX-2 primary antibody (SP21), Qubit™ RNA HS assay kit, Qubit™ RNA IQ assay kit, and primers were from Invitrogen by Thermo Fisher Scientific (Waltham, MA, USA). GAPDH rabbit monoclonal antibody and the anti-rabbit secondary antibody were obtained from Abcam. WesternBright ECL HRP substrate was from Advansta (Menlo Park, CA, USA). qScript™ cDNA SuperMix was from Quanta BioSciences, Inc. (Gaithersburg, MD, USA). NZYTaq II 2X Green Master Mix was from Nzytech (Lisbon, Portugal).

2.2. Sampling and extraction

The sampling protocol focuses on collecting plant materials (during the spring of 2019), and parameters such as plant species, growth stage, plant parts and site of the collection are presented in Table 1. Plant parts (around 10 Kg) were randomly harvested from healthy plants and collected in paper bags to avoid moisture condensation and possible damage. Plant samples were transferred immediately to the laboratory, where they were dusted off to remove any attached soil particles. Then, foreign material was eliminated. After this cleaning, plant material was spread carefully over filter paper and air dried at shade and room temperature for 15 days.

EOs were extracted by hydrodistillation; 100 g of dried plant samples were cut into 2–3 cm pieces and placed along 500 mL of distilled water in a Clevenger-type apparatus. A kinetic survey of the extraction time was done for each plant species in order to determine the optimal extraction times giving the best yields of EOs. At the end of extraction,

Table 1

Essential oil code, plant name (common name), growth stage, plant parts and sites of collection of the eight studied plants.

EO code	Plant name (common name)	Growth stage	Plant parts	Site in Tunisia	GPS coordinates
EO1	*Salvia officinalis* (sage)	Flowering	Aerial parts	Soliman	36°42′14.1″N 10°27′52.0″E
EO2	*Coriandrum sativum* (coriander)	Fructification	Mature seeds	Korba	36°33′51.0″N 10°51′27.9″E
EO3	*Rosmarinus officinalis* (rosemary)	Flowering	Aerial parts	Takelsa	36°43′39.7″N 10°38′16.8″E
EO4	*Nigella sativa* (black cumin)	Fructification	Mature seeds	Korba	36°33′51.0″N 10°51′27.9″E
EO5	*Juniperus oxycedrus* (prickly juniper)	Vegetative	Terminal branches	Beja	36°43′20.5″N 9°09′43.2″E
EO6	*Pelargonium graveolens* (geranium)	Flowering	Aerial parts	Cap Bon	37°03′20.8″N 11°01′20.3″E
EO7	*Origanum vulgare* (oregano)	Flowering	Aerial parts	Cap Bon	37°03′20.8″N 11°01′20.3″E
EO8	*Artemisia herba-alba* (wormwood)	Flowering	Aerial parts	Gabes	33°56′26.7″N 10°01′26.6″E

the recovered EOs were separated from water, dried using anhydrous Na_2SO_4 and extraction yields were calculated. The obtained EOs were stored at −20 °C in amber vials before analysis.

For the biological experiments, stock solutions were prepared by solubilizing each EO in DMSO (1:1), except for EO4, which was prepared in a proportion of (1:4) due to its worse solubility. Then, several dilutions were prepared in a cell culture medium and evaluated for their *in vitro* anti-inflammatory activity. The major components of the selected EOs were solubilized in DMSO, diluted in the cell culture medium, and tested at the same concentration that they are presented in whole EO and from which they displayed the anti-inflammatory effects. All the samples were protected from light at –20 °C until use.

2.3. Cell culture

This study was carried out on three types of cells: the HaCaT cells (ATCC, Rockville, MD, USA), which are a spontaneously immortalized human keratinocyte cell line (Boukamp et al., 1988); THP-1 cells (ATCC, LGC Standards, Spain), a human leukaemia monocytic cell line (Bosshart & Heinzelmann, 2016) and THP-1-Lucia™ NF-κB cells (InvivoGen, San Diego, CA, USA) stably transfected with a NF-κB-inducible Luc reporter construct.

The HaCaT cells were cultured in DMEM supplemented with 10 % FBS and 1 % penicillin/streptomycin. THP-1 and THP-1-Lucia™ NF-κB cells were maintained in RPMI 1640 medium, containing 10 % FBS, 1 % penicillin/streptomycin and 25 mM HEPES. In the case of THP-1-Lucia™ NF-κB cells, Normocin was added to the media at a final concentration of 100 μg/mL, and a selective antibiotic, Zeocin, was added every other passage at 100 μg/mL, as recommended by the supplier. HaCaT cells were cultured in T75 flasks at 37 °C in a humidified atmosphere of 5 % CO_2, until reach 80–90 % confluence.

2.4. Screening of EOs toxicity by MTT reduction assay

THP-1 cells were seeded at a density of 60,000 cells/well. Phorbol 12-myristate 13-acetate (PMA, 50 nM) was added as a differentiation agent to obtain macrophages, as previously described (Pech-Puch et al.,

2021). After 24 h, this medium was discarded and replaced with a fresh PMA-free medium for another 24 h period, after which the differentiated M1-macrophages were incubated with the EOs (0.03–0.5 μL/mL)/major constituents for 24 h. At the end of this period, the metabolic activity of cells was evaluated by their ability to reduce yellow tetrazolium MTT to formazan product; the wells were aspirated, and the medium was replaced with MTT at 0.5 mg/mL and incubated for 2 h. Then, the solution was discarded, and the formazan crystals dissolved in 200 μL of a DMSO:isopropanol solution (3:1). The absorbance at 560 nm was read in a Thermo Scientific Multiskan GO microplate reader. For HaCaT cells, the density used was 15,000 cells/well. Results are expressed as a percentage of the respective control and correspond to the mean ± standard error of the mean (SEM) of at least three independent experiments performed in triplicate.

2.5. Monitoring the NF-κB signal transduction pathway via THP-1-Lucia^{TM} NF-κB luciferase assay

THP-1-Lucia^{TM} NF-κB monocytes were seeded in 96-well plates and differentiated into macrophages, as described above for non-transfected THP-1 monocytes. The EOs (0.06–0.25 μL/mL)/major constituents were added, and 2 h later, LPS (1 μg/mL) was added to each well. At the end of the incubation period (22 h with LPS), 20 μL of supernatant of each well were transferred to a 96-well white plate and mixed with 50 μL of QUANTI-Luc™ assay solution, as described before (Pech-Puch et al., 2021). The plate was shaken for 15 s, and the luminescence was immediately read in a Cytation^{TM} 3 (BioTek). Results correspond to the mean ± SEM and are expressed as fold decrease *vs* LPS. Dexamethasone at 50 μM was used as a positive control.

2.6. RNA extraction, quantification, integrity, and conversion

THP-1 cells were seeded at a density of 480,000 cells/well in 12-well plates and differentiated into macrophages as described above and treated for 22 h with LPS (1 μg/mL), with or without pre-incubation with the selected EOs (0.125 or 0.25 μL/mL)/major constituents for 2 h. Afterwards, the supernatant was removed to be used in ELISA, and the cells were disrupted in 500 μL of PureZOL reagent to perform the RNA extraction as described before (Pech-Puch et al., 2021; Pereira et al., 2019). Briefly, the cell samples in PureZOL were transferred to a RNase-free tube, and 100 μL of chloroform were added. The mixture was shaken vigorously for 15 s. After 5 min incubation at room temperature, the samples were centrifuged at 12,000 × *g* for 15 min at 4 °C. Following centrifugation, the aqueous phase containing the RNA was immediately transferred to a new RNase-free tube, and 250 μL of isopropyl alcohol were added. The mixture was then incubated at room temperature for 5 min. Afterwards, the tubes were centrifuged at 12,000 × *g* for 10 min at 4 °C, the RNA appearing as a white pellet on the side and bottom of the tube. The supernatant was carefully discarded, and the RNA pellet was washed with 1 mL of 75 % ethanol. After vortexing, the mixture was centrifuged at 7500 × *g* for 5 min at 4 °C, and the supernatant was carefully discarded. Then, the RNA pellet was air-dried for about 5 min and reconstituted in 25 μL of PCR grade water. Subsequently, the RNA was quantified using the Qubit^{TM} RNA HS assay kit in a Qubit 4 fluorometer (Invitrogen by Thermo Fisher Scientific; Waltham, MA, USA). The RNA quality and integrity were evaluated using the Qubit RNA^{TM} IQ assay kit. 1 μg of RNA was mixed with 4 μL qScript cDNA SuperMix (Quanta BioSciences, Inc.) in a 20-μL reaction to obtain the complementary DNA. The reverse-transcribed reaction involved three steps: 5 min at 25 °C, 30 min at 42 °C, and 5 min at 85 °C.

2.7. qPCR analysis

q-PCR analyses were conducted on multiple target genes, namely COX-2, TNF-α, IL-6, and IL-1β. GAPDH was used as a reference gene. The primers were designed using the Primer-BLAST tool (NCBI, Bethesda,

MD, USA) and synthesized by Thermo Fisher (Waltham, MA, USA), as listed in Supplementary Table S1.

Real-time qPCR was performed with 5 ng of cDNA using NZYTaq II 2X Green Master Mix, similar to what we described before (Pech-Puch et al., 2021; Pereira et al., 2019). The thermal cycling conditions were as follows: 3 min at 95 °C, followed by 40 cycles of denaturation at 95 °C for 3 s, specific annealing temperatures for each gene for 20 s, and extension at 72 °C for 20 s. The fluorescence signal was detected at the end of each cycle. The results were analyzed with qPCRsoft 4.0 supplied with the equipment qTOWER3 G (Analytik Jena AG, Germany), and a melting curve was used to confirm the specificity of the products. Transcript abundances of the target genes were normalized to the expression of GAPDH (reference gene). Samples were run in duplicate in each PCR assay. Normalized expression values were calculated following the mathematical model proposed by Pfaffl using the formula: $2^{-\Delta\Delta Ct}$, where $\Delta\Delta Ct$ = (Ct target gene – Ct GAPDH) $_{treatment}$ – (Ct target gene – Ct GAPDH) $_{control}$. Results correspond to the mean ± SEM and are expressed as fold decrease *vs* LPS. At least three independent experiments were performed. Dexamethasone at 50 μM was used as a positive control.

2.8. Enzyme-Linked immunosorbent assay (ELISA)

THP-1 monocytes were seeded in 12-well plates, differentiated into macrophages, and treated, as described above, for RNA extraction, quantification, integrity, and conversion. The concentrations of the pro-inflammatory cytokines IL-6, TNF-α and IL-1β were determined in the supernatants using an ELISA kit, according to the manufacturer's instructions (BioLegend Inc.; San Diego, CA, USA). Results correspond to the mean ± SEM of at least three independent experiments and are expressed as fold decrease *vs* LPS. Dexamethasone at 50 μM was used as a positive control.

2.9. Detection of cyclooxygenase 2 (COX-2) protein expression

Western blot analysis was carried out using a previously described method (Pereira et al., 2019), with some modifications. Briefly, THP-1 cells (480000 cells/well) were seeded in 12-well plates and treated for 22 h with LPS (1 μg/mL), with or without pre-incubation with EOs/major constituents for 2 h. After treatment, cells were washed with HBSS, scraped, and incubated with RIPA lysis buffer containing 1 % of protease inhibitor cocktail, on ice, for 30 min. Then, cell debris were removed by microcentrifugation (14,000 × *g* for 15 min), and supernatants were rapidly frozen at –80 °C. Protein concentrations were determined using Qubit^{TM} Protein Assay Kit according to the manufacturer's instructions. Proteins (30 μg) were separated on 10 % sodium dodecylsulphate (SDS)-polyacrylamide minigels and transferred onto nitrocellulose membranes (Bio-Rad, USA) that were subsequently blocked for 1 h at room temperature with a solution of 5 % skimmed milk powder in PBS 0.1 % Triton X-100. The membranes were incubated overnight at 4 °C with specific antibodies against COX-2 (1:500) or GAPDH (1:10000). After washing, membranes were incubated with secondary antibody (1:3000) at room temperature for 2 h, followed by the addition of ECL reagent. The relative optical density of bands was quantified by densitometry and normalized with respect to GAPDH (loading control). The results correspond to the mean ± SEM of three independent experiments. Dexamethasone at 50 μM was used as a positive control.

2.10. Caspase-Glo® 1 inflammasome assay

THP-1 cells were cultured and differentiated in a 96-well white plate (60000 cells/well), as described above for the MTT assay. After this period, cells were treated for 2 h with LPS (1 μg/mL), with or without pre-incubation with EOs/major constituents for 2 h, at 37 °C. O'Brien et al., 2017 have demonstrated that the maximal caspase-1 activity was

achieved after 2 h stimulation with LPS). Then, 50 μL of cell culture medium was removed from each well, and 50 μL of Caspase-Glo® 1 reagent or Caspase-Glo® 1 YVAD-CHO reagent was added to the wells, according to the manufacturer's instructions (Promega Corporation, Fitchburg, WI, USA). The luminescent signal was determined after incubation for 90 min in a microplate reader (Cytation™ 3, BioTek). Results correspond to the fold-decrease of luminescence in treated *vs* LPS cells of three independent experiments performed in duplicate. Dexamethasone at 50 μM was used for comparison purposes.

2.11. GC–MS analysis

The chemical composition of studied EOs (*Coriandrum sativum* (coriander), *Pelargonium graveolens* (geranium) and *Artemisia herba-alba* (wormwood)) was determined by gas chromatography (Agilent 7890 A Agilent, Waldbronn, Germany) coupled to mass spectrometry (Agilent 5975C Agilent, Waldbronn, Germany), mass spectrometer with electron impact ionization (70 eV). An apolar HP-5MS capillary column (30 m × 0.25 mm coated with 5 % phenyl methylsilicone and 95 % dimethyl polysiloxane, 0.25 μm film thickness) was used. The oven temperature was programmed to rise from 50 °C to 240 °C at a rate of 5 °C/min. The injector and detector temperatures were respectively equal to 250 and 325 °C. The carrier gas was helium with a flow rate of 1.2 mL/min; the injection volume was 1 μL and the split ratio was 60:1. Scan time and mass range were 1 s and 40–300 *m/z*, respectively.

EOs volatile compounds were identified by comparing their retention indexes (RI) related to (C9–C18) *n*-alkanes with those of authentic compounds (Analytical reagents, LabScan, ltd, Dublin, Ireland) available in the literature and in our laboratory and by matching their mass spectra fragmentation patterns with corresponding data stored in the mass spectra library of the GC–MS data system (NIST) and other published mass spectra (Adams, 2005). Relative percentage amounts of the identified compounds were obtained from the electronic integration of the FID peak area. All analyses were repeated three times, and the results represent mean values ± standard deviation. The percentage of compounds was calculated using HP-Chemstation software based on their respective areas.
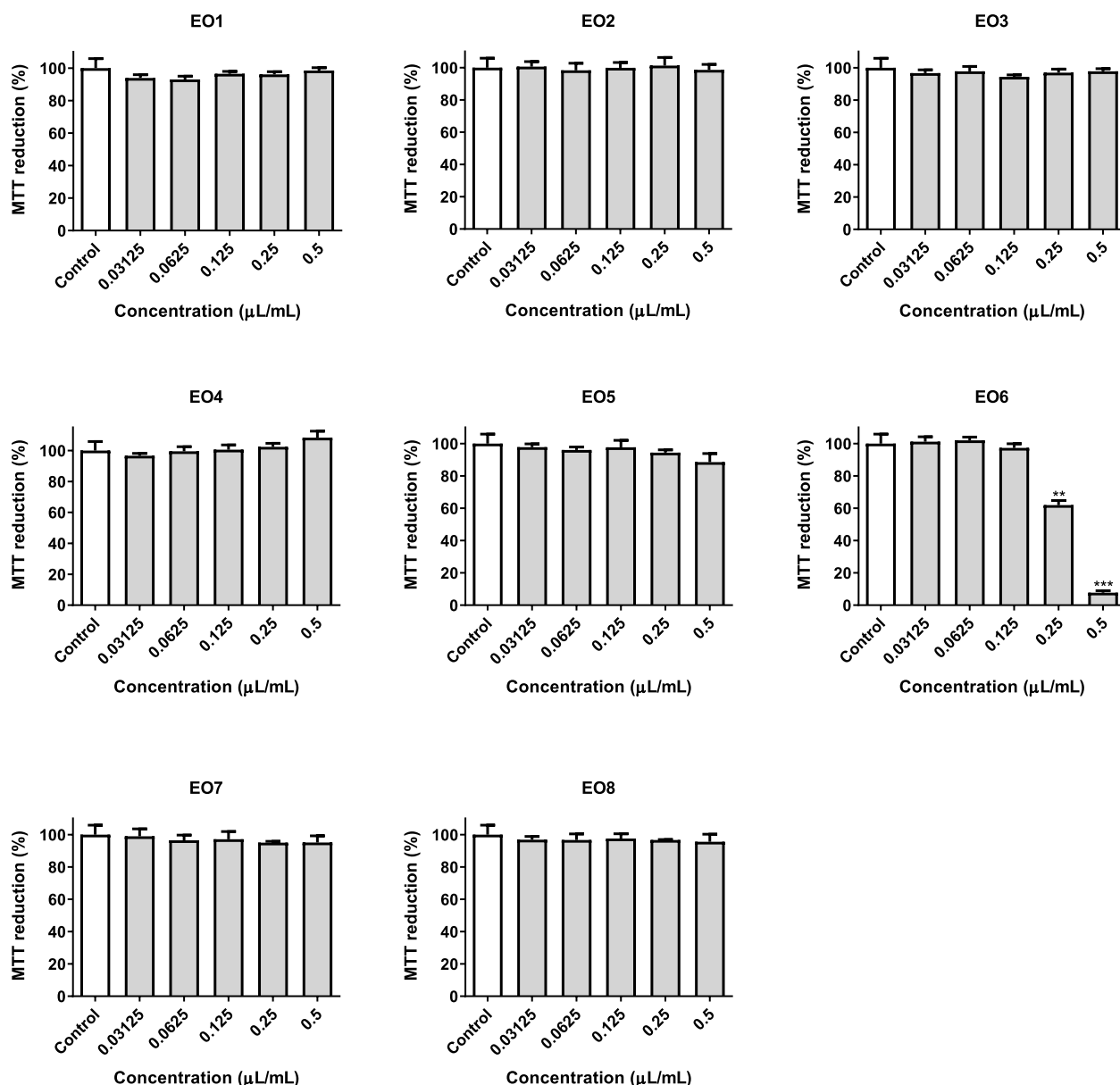

Fig. 1. Viability of THP-1 macrophages treated with increasing concentrations of eight EOs (EO1-8), as assessed by the MTT assay. ** $p < 0.01$, *** $p < 0.001$.

2.12. Statistical analysis

Data analysis was performed using GraphPad Prism 6.01 Software (San Diego, CA, USA). Grubbs' test was used to detect and exclude outliers. Before the analysis, the data set was checked for normality of distribution using the Shapiro–Wilk test, ensuring that all data followed a normal distribution. Levels of significance were determined using an unpaired Student's *t*-test where each column of treatment was compared to the control. All data were expressed as mean ± SEM of at least three independent experiments performed in triplicate. Values of $p < 0.05$ were considered statistically significant.

3. Results and discussion

3.1. Anti-inflammatory activity of EOs

The eight EO samples were tested for their toxicity towards THP-1 macrophages, by evaluating their direct effects on cell viability, within a concentration range from 0.03 to 0.5 μL/mL (Fig. 1). This is a crucial step, as it allows the removal of toxic concentrations that could negatively impact subsequent assays, highlighting as well the importance of using distinct working concentrations depending on the sample. Due to

the recognized contact allergy caused by some EOs if used on the skin (De Groot & Schmidt, 2016; Sindle & Martin, 2021), all the samples were also evaluated for their toxicity against human keratinocytes (HaCaT cells). As can be seen, all the EOs tested, apart from EO6, were non-toxic to HaCaT cells at concentrations equal to or lower than 0.25 μL/mL (Supplementary Fig. S1). Furthermore, all EOs tested were generally less toxic to macrophages than to keratinocytes (Fig. 1 and supplementary Fig. S1). However, in our study, for the NF-κB activation assay, we selected the two non-toxic concentrations based on the cytotoxicity to both cell lines (THP-1 and HaCaT cells) which corresponds to 0.125 and 0.25 μL/mL for all EOs, apart from EO6, which was the most cytotoxic, as previously shown. Therefore, for EO6 lower concentrations were screened.

After selecting the non-cytotoxic concentrations, all samples were assessed for their ability to prevent or ameliorate the activation of the nuclear factor-κB (NF-κB) pathway in LPS-challenged cells (Fig. 2). This pathway comprises a set of key events for the inflammatory process, being frequently upstream of other genetic and phenotypic changes. NF-κB represents a family of inducible transcription factors involved in different processes of the immune and inflammatory responses (Liu, Zhang, Joo, & Sun, 2017). It controls many genes involved in the pathogenesis of several inflammatory diseases, such as multiple
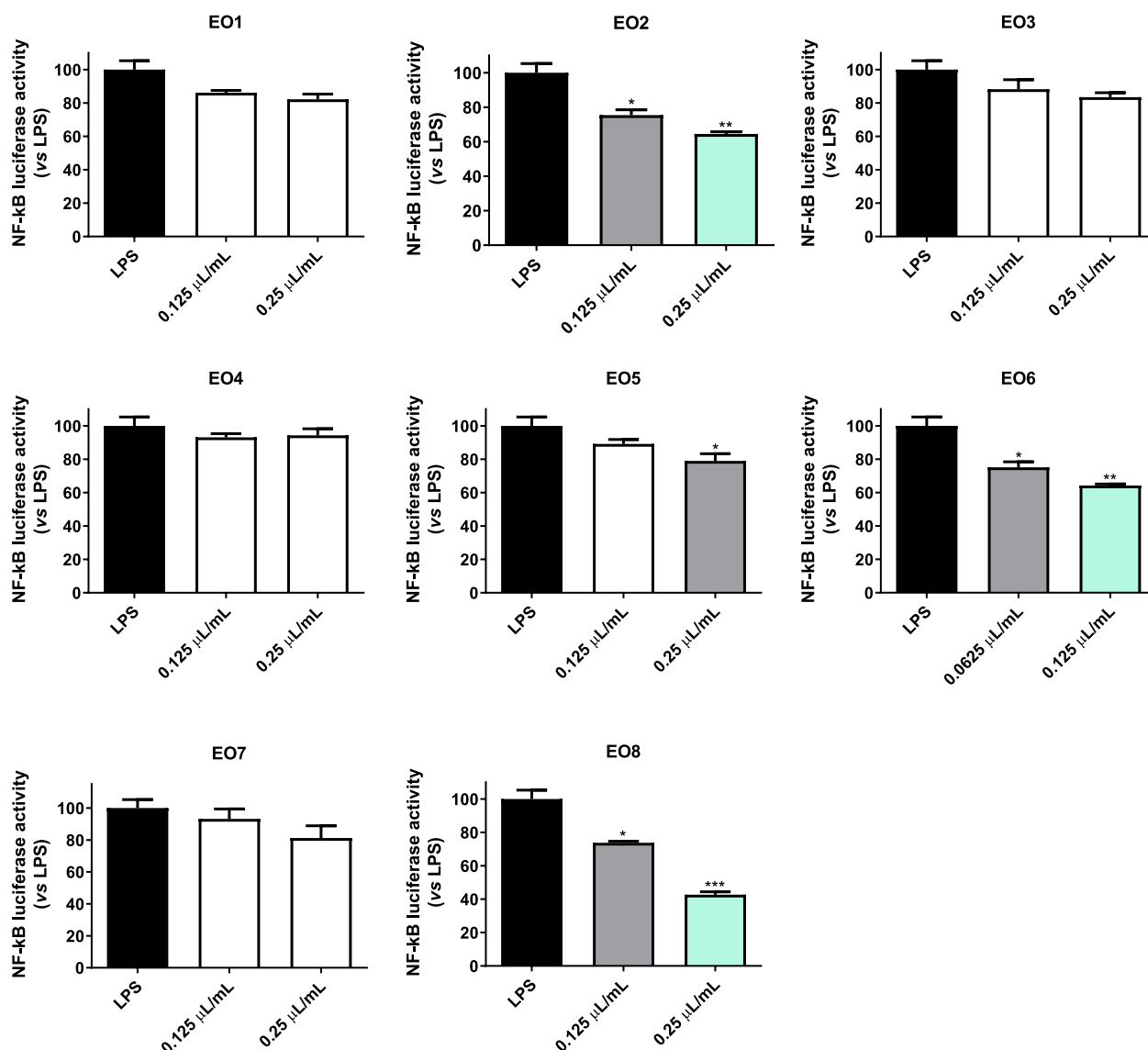
Fig. 2. NF-κB activation status of THP-1 luciferase reporter-transfected cells for the different samples. * $p < 0.05$, ** $p < 0.01$, *** $p < 0.001$.

sclerosis, atherosclerosis, asthma, inflammatory bowel disease and rheumatoid arthritis, being therefore considered an attractive target for new anti-inflammatory drugs (Liu et al., 2017; Park & Hong, 2016). The experimental model uses THP-1-Lucia™ NF-κB cells derived from the human THP-1 monocyte cell line by the stable integration of an NF-κB-inducible Lucia™ reporter construct. In this model, LPS-mediated NF-κB pathway activation results in luciferase being produced and released to the cell culture media, allowing the monitoring of NF-κB activation by determining luciferase activity. Among the eight EOs tested, three (EO2 - *Coriandrum sativum*, EO6 - *Pelargonium graveolens* and EO8 - *Artemisia herba-alba*) were able to significantly prevent the activation of this pathway, in some cases by over 50 % (Fig. 2). These are promising results, as they suggest these specific EOs may have a relevant role in the modulation of the inflammatory process, by containing potential new modulators of the NF-κB pathway.

After the capacity of EO2, EO6 and EO8 to negatively modulate the activation of the NF-κB pathway had been identified, we were interested in assessing the putative target genes involved in this effect. To this end, the three samples were selected for subsequent studies. Specifically, we collected RNA from EO-treated cells in the presence of the pro-inflammatory molecule LPS. This RNA was then converted into cDNA, and the samples' effect on the expression of NF-κB dependent target genes such as IL-6, IL-1β, TNF-α and COX-2 was evaluated. As shown in Fig. 3A, all samples were able to significantly lower the expression of these genes, demonstrating their capacity to interfere in the inflammatory process. Of note, for all the analysed EOs, the protein levels of IL-6, TNF-α and COX-2 were associated with their respective mRNA expression (Fig. 3B). Differently, in the case of IL-1β, the simultaneous downregulation of mRNA and protein levels have only been observed for EO2 and EO8, the latter eliciting a marked decrease in protein level (Fig. 3B).

One downstream player in the NF-κB pathway is the NLRP3 inflammasome, a protein complex that is activated through the NF-κB-associated induction of its transcriptional expression and licensing of IL-1β mRNA synthesis and later activation of caspase-1 (Tran et al., 2019). Considering that the production and release of mature IL-1β to the cell culture medium is closely related to caspase-1 activity, the effect of the selected EOs in caspase-1 activation was screened. As shown in Fig. 4, EO8 displayed a strong inhibition of caspase-1, which is consistent with the marked decrease caused in mature IL-1β levels (Fig. 3B). Similarly, EO2 exhibiting nearly 50 % of caspase-1 inhibition also significantly reduced IL-1β levels (Fig. 3B and 4). On the other hand, EO6, which also demonstrated the ability to inhibit caspase-1, did not show any significant decrease of LPS-induced IL-1β protein levels in THP-1 macrophages (Fig. 3B and 4). To explain this, it is important to note that, despite all the selected EOs downregulate the NF-κB pathway, therefore decreasing IL-6, IL-1β, TNF-α and COX-2 mRNA expression, the release of IL-1β is dependent on the processing rate of pro-IL-1β to IL-1β by caspase-1 (Huang et al. 2021). As so, once caspase-1 activity was measured after 2 h exposure to LPS and the IL-1β protein expression was determined after 22 h exposure, this effect may result from events occurring across this period (e.g., a reversion of the caspase-1 inhibitory capacity).

3.2. Major constituents can mimic the anti-inflammatory activity of the whole EO

Once the most promising EOs have been selected and explored from a mechanistic point of view, we were interested in investigating the chemical composition of these samples to establish a relationship between the compounds presented in each EO and the anti-inflammatory activity reported herein. With this aim in view, EO2 - *Coriandrum sativum*, EO6 - *Pelargonium graveolens* and EO8 - *Artemisia herba-alba* were analysed by GC–MS, the chemical composition being reported in Table 2. Chromatograms can be found in supplementary Fig. S2.

There are few studies in the literature reporting anti-inflammatory properties of the major components in THP-1 macrophages. Once

information regarding the anti-inflammatory activity of the major constituents in our cell model is scarce, we intended to screen the anti-inflammatory properties of the major components of each EO. To this end, the two major constituents (>50 % of each EO) were screened alone and in binary mixtures at the same concentrations that they are presented in whole EO and from which they displayed the above-mentioned anti-inflammatory effects (i.e., EO2 (Lin – 140.51 μg/mL; α-pinene – 15.91 μg/mL); EO6 (β-cit – 40.98 μg/mL; Ger – 16.69 μg/mL); EO8 (α-Thuj – 90.70 μg/mL; CPO – 28.16 μg/mL)). The concentration of the major components was determined based on their relative percentage (Table 2) and each EO density. It is important to mention that β-thujone is not commercially available in its pure form but in a mixture with α-thujone (~70 % α-thujone basis, ~10 % β-thujone basis). For this reason, in the case of EO8, which has β-thujone as a major component, α-thujone was used. Considering the chemical complexity of each EO, potential synergistic and antagonistic effects could occur among the components, affecting positively or negatively the toxicity of each EO, as well as its anti-inflammatory properties. To ensure that the major components and binary mixtures are non-toxic to THP-1 macrophages, viability studies were conducted following the same procedures described for the crude EOs. As shown in Fig. 5A, none of the major constituents of the selected EOs and/or binary mixtures significantly decrease the viability of THP-1 macrophages.

After ensuring that the major constituents and/or binary mixtures were devoid of toxicity to THP-1 macrophages, the samples were screened in the same model described above using the THP-1-Lucia™ NF-κB cells (Fig. 5B). In the case of EO2 and EO6, the major components linalool and β-citronellol mimicked the NF-κB inhibition reported above for the crude EOs (Figs. 2 and 5B). Previous studies have reported the capacity of linalool to protect renal function alleviating inflammation due to injury in mice by reducing the expression of TLR4 (LPS receptor), MyD88, and TRAF and attenuating the release of pro-inflammatory cytokines like TNF- α, IL-1β, and IL-6 (Mohamed et al., 2020). Similarly, Jayaganesh et al. (2020) demonstrated that the oral administration of citronellol to DMBA-treated rats significantly downregulated the expression of NF-κB65, TNF-α, IL-6, COX-2 and iNOS (Jayaganesh et al. 2020). Further, linalool ameliorates lung inflammation and excess mucus secretion by downregulating the NF- κB signalling pathway, which is in line with our findings (Kim et al., 2020). Noteworthy, the second major component of EO2 and EO6, α-pinene and geraniol, were completely devoid of activity (Fig. 5B). α-pinene (100 μg/mL) was reported to have the capacity to decrease the NF-κB/p65 nuclear translocation, promoting cytoplasmic IκB-α accumulation in the same cell model used in our work (Zhou, Tang, Mao, & Bian, 2004) and despite its presence in a lower amount in EO2 (15.91 μg/mL) it may contribute to the observed effect. In addition, no significant differences have been found in the NF-κB luciferase activity between the major component of EO2 (linalool) and EO6 (β-citronellol) and their binary mixtures with α-pinene and geraniol, respectively (Fig. 5B). Contrarily, when the major components of EO8 were tested alone, no significant impact on NF-κB activation was evidenced (Fig. 5B). On the other hand, the binary mixture of α-thujone and camphor seemed to display a synergistic effect, significantly decreasing NF-κB activation (Fig. 5B), nevertheless in a lower extension than the crude EO8 (Fig. 2). Considering all these results, in the case of EO2 and EO6, additional studies related to the expression of pro-inflammatory genes and proteins were conducted with the major components linalool and β-citronellol, respectively. In contrast, for EO8, the binary mixture of the two major components were used once each compound individually was completely devoid of activity (Fig. 5B).

qPCR analyses revealed that the levels of IL-6, IL-1β, TNF-α and COX-2 mRNA expression were significantly reduced in THP-1 macrophages after treatment with the major components (Fig. 6A). Remarkably, linalool, the major component of EO2 constituting *ca* 65 % of total volatiles, decreased the expression of all pro-inflammatory genes tested in a higher extension than the crude EO2 (Fig. 3A and 6A). In agreement,
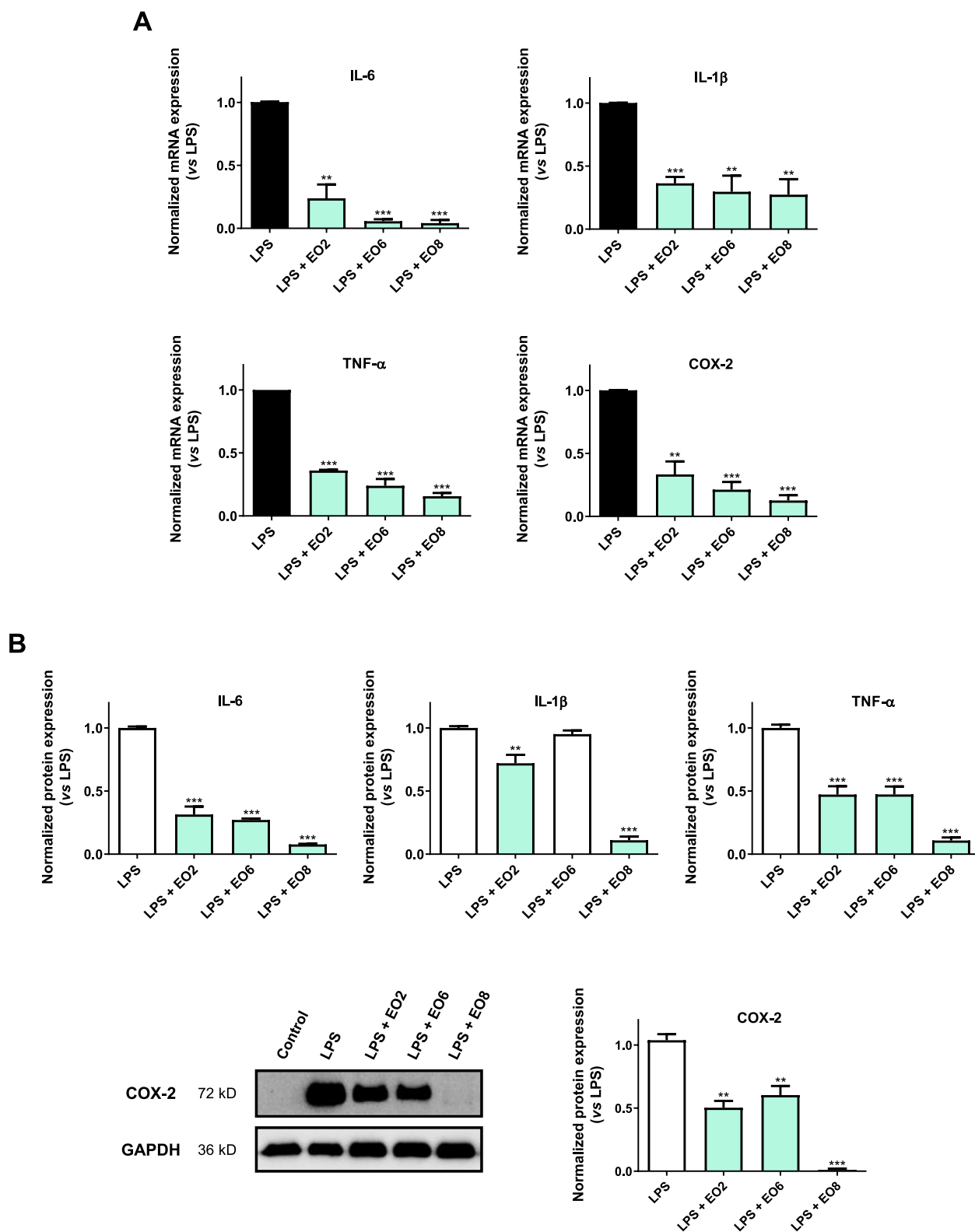
Fig. 3. (A) Effect of selected EOs on LPS-induced IL-6, IL-1β, TNF-α and COX-2 mRNA expression. qPCR data were normalized to the reference gene, GAPDH. (B) Effect of selected EOs on LPS-induced IL-6, IL-1β, TNF-α and COX-2 protein expression. THP-1 macrophages were treated for 22 h with LPS (1 μg/mL), with or without pre-incubation with the selected EOs for 2 h. **LPS:** lipopolysaccharide; **EO2:** *Coriandrum sativum* at 0.25 μL/mL; **EO6:** *Pelargonium graveolens* at 0.125 μL/mL; **EO8:** *Artemisia herba-alba* at 0.25 μL/mL. ** $p < 0.01$, *** $p < 0.001$.
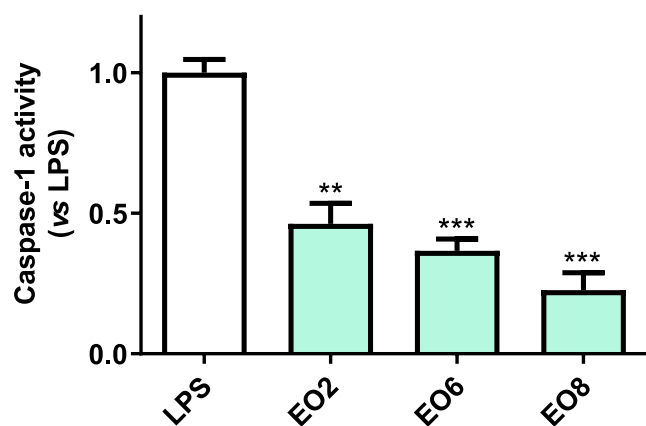
Fig. 4. Effect of selected EOs on caspase-1 inflammasome activation in THP-1 macrophages. Data represent the mean ± SEM of three independent experiments performed in duplicate. THP-1 macrophages were treated for 2 h with LPS (1 μg/mL), with or without pre-incubation with the selected EOs for 2 h. **LPS:** lipopolysaccharide; **EO2:** *Coriandrum sativum* at 0.25 μL/mL; **EO6:** *Pelargonium graveolens* at 0.125 μL/mL; **EO8:** *Artemisia herba-alba* at 0.25 μL/mL. ** $p < 0.01$, *** $p < 0.001$.

previous studies have demonstrated the ability of linalool to inhibit endotoxin-induced TNF-α and IL-1β in RAW macrophages (Huo et al., 2013) and in BV2 cells (Li et al., 2015). Noteworthy, the major components of each EO under study mimic the effect of the crude EOs on the COX-2 mRNA expression (Fig. 3A and 6A). On the other hand, despite the significant differences being found in the IL-6 mRNA expression upon treatment with the major constituents, the effect of the crude EOs was more pronounced. The same behaviour was also evidenced when comparing the decrease of TNF-α mRNA expressions caused by EO6 and EO8 with those achieved by β-citronellol and the binary mixture α-thujone plus camphor, respectively (Fig. 3A and 6A). These results can be explained by the presence of bioactive minor components in the crude EOs, as well as by synergistic effects that may take place in this complex mixture. Regarding protein expression, the IL-6, IL-1β (except after β-citronellol treatment), TNF-α and COX-2 levels were significantly decreased by major constituents, aligned with the mRNA expressions (Fig. 6). In line with our findings, Su et al., 2010 showed that β-citronellol attenuate mRNA and protein expression of COX-2 induced by LPS through a reversion in the the cytoplasmic degradation of IκB-α and the upregulation of NF-κB in the nucleus of murine macrophages (Su, Chao, Lee, Ou, & Tsai, 2010). It has been also described before that linalool is capable of downregulating COX-2 expression in skin a model of UVB-mediated aggression, being also suggested that the hydrogen-donating ability of linalool is correlated with this effect (Gunaseelan et al. 2016). Of note, the ability of β-citronellol to downregulate COX-2 has also been described in several cell types and models (Su, Chao, Lee, Ou, & Tsai, 2010; Santos et al., 2021). The precise mechanism by which this occurs has not been reported. In addition, thujone and camphor displayed the ability to decrease the release of IL-6 and IL-8 in PMA/ionomycin stimulated HGF-1 cells (Ehrnhöfer-Ressler et al., 2013). Furthermore, an *Artemisia fukudo* EO having α-thujone as the major compound (nearly 50 %) shown the ability to inhibit LPS-induced phosphorylation and degradation of IκB-α, an event required for the nuclear translocation of NF-κB (Yoon et al., 2010). Lastly, it is important to note that although the anti-inflammatory properties reported in the literature for the major compounds may explain our findings, the contribution of the minor components to the observed effects cannot be neglected. Moreover, as the EOs presented herein are composed of at least fifteen volatile compounds, synergistic effects between the different molecules cannot be excluded and may explain the observed anti-inflammatory activity.

Concerning caspase-1 inflammasome assay, β-citronellol, the major

Table 2
Chemical composition of coriander (EO2), geranium (EO6) and wormwood (EO8) essential oils. Chromatograms can be found in supplementary Fig. S2.

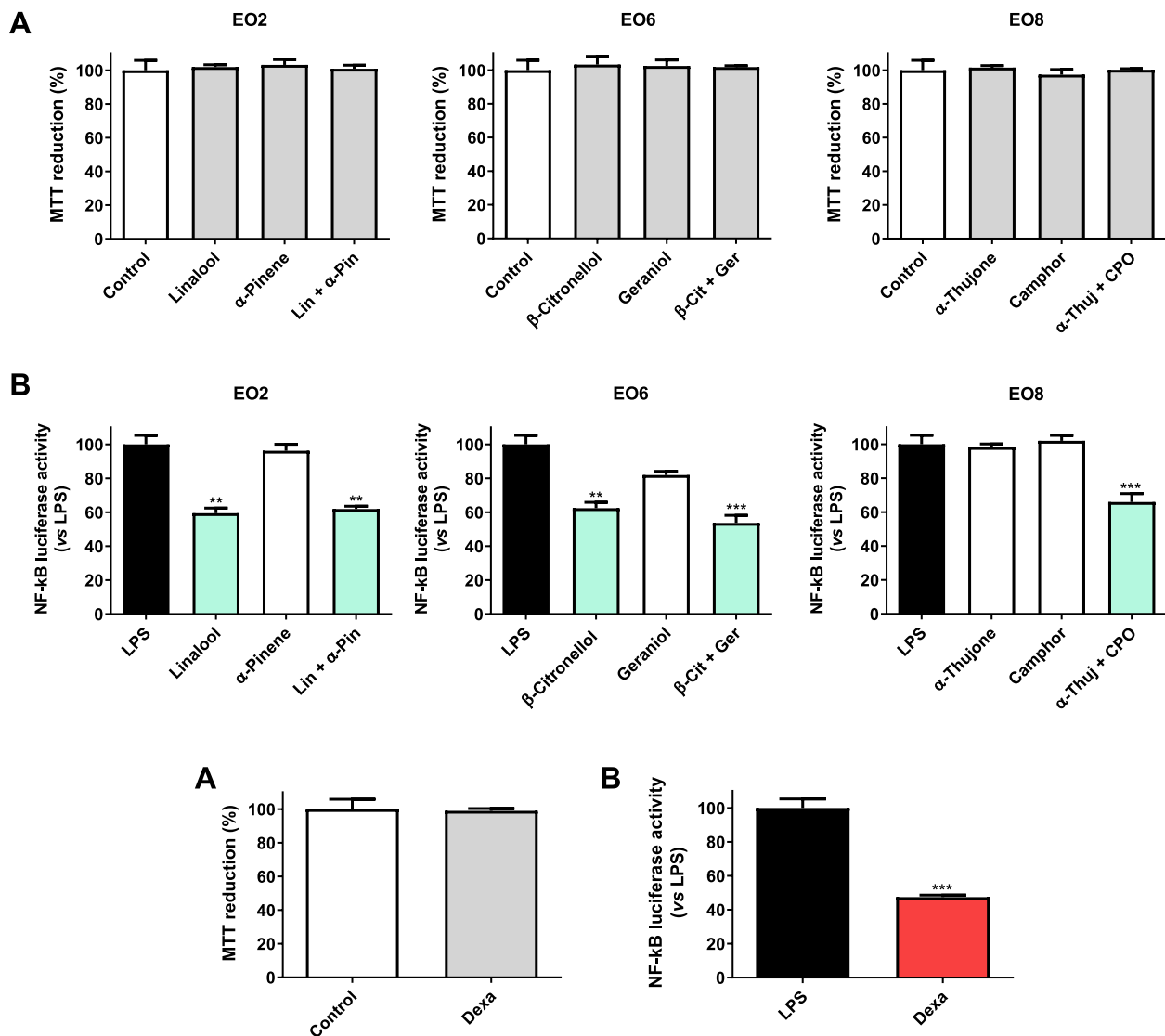| RI	Compound (%)	*C. sativum* (EO2)	*P. graveolens* (EO6)	*A. herba-alba* (EO8)
856	Butanoic acid	–	1.00 ± 0.05	–
939	**α-pinene**	**7.26 ± 0.22**	0.63 ± 0.03	–
954	Camphene	1.23 ± 0.07	–	1.38 ± 0.06
975	Sabinene	0.29 ± 0.01	–	–
980	β-pinene	0.48 ± 0.03	–	–
991	β-myrcene	0.63 ± 0.05	–	–
1026	*p*-cymene	–	–	0.89 ± 0.03
1028	*o*-Cymene	5.91 ± 0.15	–	–
1030	ᴅ-limonene	3.02 ± 0.09	–	–
1033	1,8-cineole	–	–	5.69 ± 0.11
1062	γ-terpinene	2.94 ± 0.09	–	–
1088	*Trans* linalool oxide	3.53 ± 0.12	–	–
1098	**Linalool**	**64.10 ± 0.68**	4.59 ± 0.08	–
1105	α-Thujone	–	–	11.58 ± 0.17
1106	Filifolone	–	–	1.97 ± 0.07
1114	**β-thujone**	–	–	**38.27 ± 0.53**
1117	Rose oxide	–	1.31 ± 0.05	–
1124	Chrysanthenone	–	–	6.76 ± 0.10
1136	1-terpineol	–	–	0.67 ± 0.02
1140	**Camphor**	5.50 ± 0.12	–	**11.88 ± 0.20**
1143	*Trans*-Verbenol	–	–	1.77 ± 0.05
1144	4-Terpineol	–	–	0.75 ± 0.03
1150	Pinocarvone	–	–	0.71 ± 0.04
1154	Menthone	–	5.67 ± 0.092	–
1165	*endo*-Borneol	–	–	2.07 ± 0.06
1180	*Trans*-1,2-Dihydroperillaldehyde	–	–	0.73 ± 0.08
1199	Terpendiol	0.37 ± 0.03	–	–
1207	α-terpineol	0.62 ± 0.05	–	–
1233	**β-citronellol**	–	**36.88 ± 0.45**	–
1240	α-citral	–	0.6 ± 0.02	–
1251	Piperitone	–	–	0.60 ± 0.01
1275	Citronellyl formate	–	8.74 ± 0.10	–
1276	**Geraniol**	0.78 ± 0.06	**15.02 ± 0.16**	–
1285	Bornyl acetate	–	–	5.08 ± 0.09
1292	Sabinyl acetate	–	–	7.24 ± 0.10
1351	α-cubebene	–	0.61 ± 0.02	–
1380	β-bourbonene	–	1.64 ± 0.06	–
1383	Geranyl acetate	3.35 ± 0.10	0.74 ± 0.03	–
1391	α-copaene	–	0.64 ± 0.03	–
1494	Bicyclogermacrene	–	–	0.64 ± 0.01
1499	Germacrene-D	–	1.53 ± 0.06	0.90 ± 0.03
1530	δ-cadinene	–	2.25 ± 0.06	–
1584	Phenyl tiglate 2	–	1.40 ± 0.06	–
1602	8-*epi*-γ-eudesmol	–	6.40 ± 0.09	–
1618	Caryophyllene	–	1.65 ± 0.06	–
1650	Indene	–	1.18 ± 0.06	–
1700	Geranyl tiglate	–	1.39 ± 0.05	–
1717	Geraniol formate	–	3.22 ± 0.07	–

Fig. 5. (A) Viability of THP-1 macrophages treated with the major constituents of EO2, EO6 and EO8, as assessed by the MTT assay. (B) NF-κB activation status of THP-1 luciferase reporter-transfected cells for the major constituents of EO2, EO6 and EO8. **LPS**: lipopolysaccharide; **Lin**: Linalool; **α-Pin**: α-Pinene; **β-Cit**: β-Citronellol; **Ger**: Geraniol; **α-Thuj**: α-Thujone; **CPO**: Camphor; **Dexa**: Dexamethasone (50 μM). ** $p < 0.01$, *** $p < 0.001$.

constituent of EO6, was the only molecule that could reduce *ca* 40 % the caspase-1 activity (Fig. 7), explaining probably the inhibition displayed by EO6 (Fig. 4). On the other hand, comparing the caspase-1 inhibitory activity of EO2 and EO8 (Fig. 4) with the activity displayed by their major constituents (Fig. 7), none of them could mimic the effect reported above for the crude EOs, suggesting, beyond possible synergistic effects, the presence of minor compounds in the crude EOs with caspase-1 inhibitory properties. Indeed, studies carried out with *Blumea balsamifera* EO containing borneol (minor component of EO8) significantly inhibits the activation of the NLRP3 inflammasome and regulates LPS-induced inflammation along with the NF-κB signaling pathway (Liao et al., 2021). Furthermore, Chen et al., 2021 also showed that *Artemisia argyi* EO containing terpinen-4-ol, 1,8-cineole and borneol, all minor components of EO8, displayed the capacity to inhibit the activation and nuclear translocation of NF-κB p65 and to suppress the caspase-1 and IL-1β processing, thereby attenuating the activation of NLRP3 inflammasome in PMA-induced THP-1 cells (Chen et al. 2021). Surprisingly, the major constituents which do not affect caspase-1 activity were those that inhibited significantly IL-1β protein expression (Fig. 6B and 7). This result was not expected since caspase-1 is responsible for the conversion of pro-IL-1β to its mature form. However, despite the different

timepoints of LPS exposure (2 h *vs* 22 h) in both assays mentioned above, the decrease in IL-1β protein levels without caspase-1 inhibition can be explained by a decrease in pro-IL-1β production, once these major constituents are NF-κB blockers (Fig. 5B).

4. Conclusions

This work reports the anti-inflammatory activity of eight EOs, *Coriandrum sativum*, *Pelargonium graveolens* and *Artemisia herba-alba* EOs being the most active, inhibiting NF-κB activation and downregulating IL-6, IL-1β, TNF-α and COX-2 mRNA expression. Furthermore, the study carried out with the major constituents of each EO revealed that the major compound or the binary mixture of the two major compounds (commercially available) are able to induce the anti-inflammatory effects reported to the crude EOs, in some cases mimicking their effect completely. Considering the low yield/chemical variability often associated with the obtention/composition of EOs, these findings assume extreme relevance. On the other hand, the ability to inhibit caspase-1 activity displayed by the same EOs was not justified by the major constituents (except for β-citronellol/EO6), suggesting, in addition to potential synergistic effects, the presence of minor compounds with
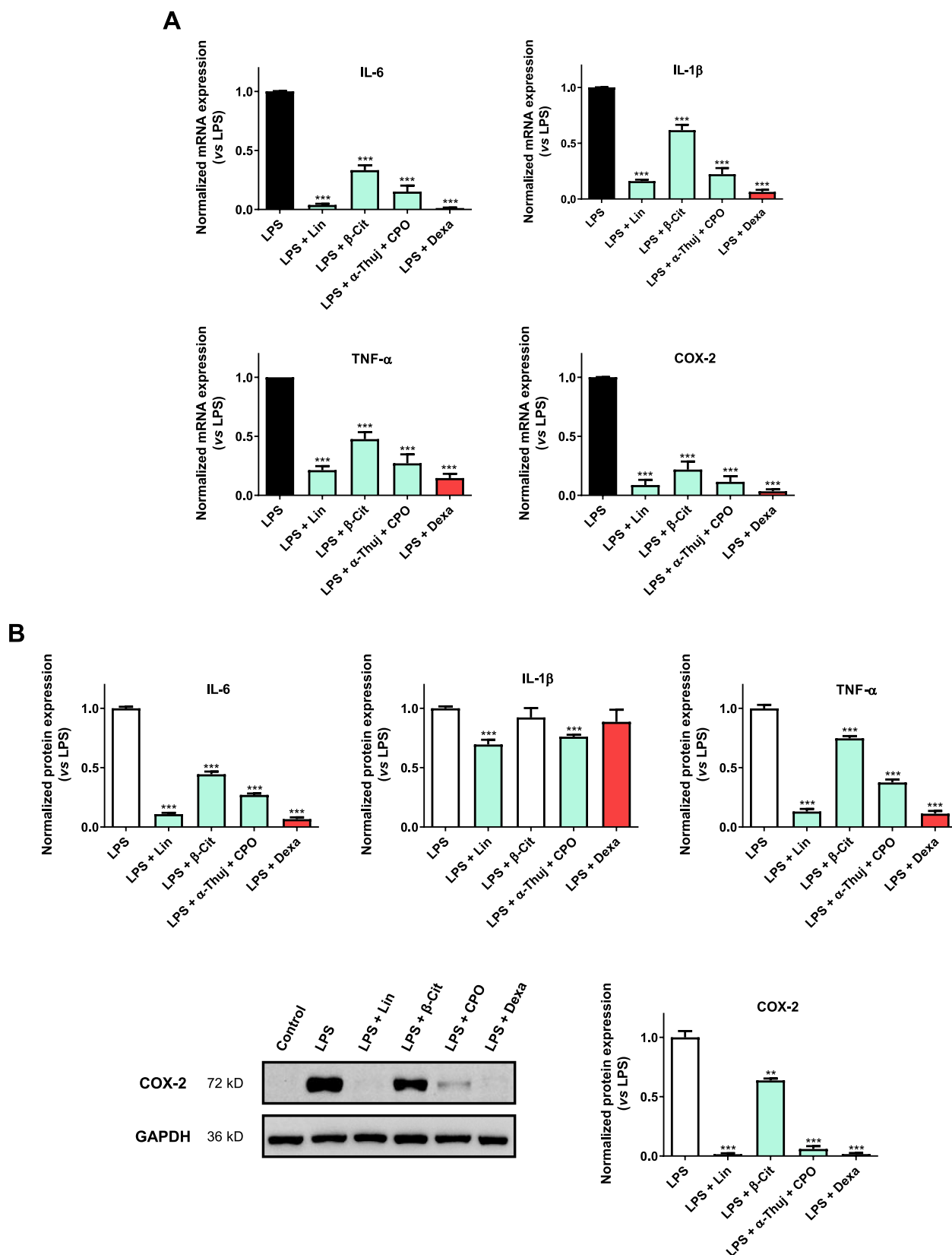
Fig. 6. (A) Effect of major constituents of EO2, EO6 and EO8 on LPS-induced IL-6, IL-1β, TNF-α and COX-2 mRNA expression. qPCR data were normalized to the reference gene, GAPDH. (B) Effect of major constituents of EO2, EO6 and EO8 on LPS-induced IL-6, IL-1β, TNF-α and COX-2 protein expression. THP-1 macrophages were treated for 22 h with LPS (1 μg/mL), with or without pre-incubation with the major constituents of selected EOs for 2 h. **LPS**: lipopolysaccharide; **Lin**: Linalool; **β-Cit**: β-Citronellol; **α-Thuj**: α-Thujone; **CPO**: Camphor; **Dexa**: Dexamethasone (50 μM). ** $p < 0.01$, *** $p < 0.001$.
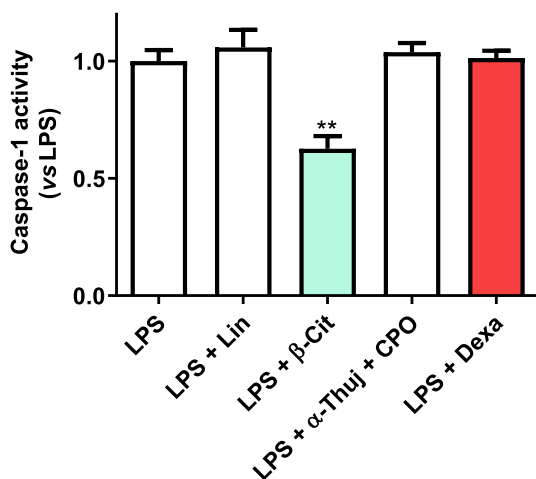
Fig. 7. Effect of major constituents of EO2, EO6 and EO8 on caspase-1 inflammasome activation in THP-1 macrophages. Data represent the mean ± SEM of three independent experiments performed in duplicate. THP-1 macrophages were treated for 2 h with LPS (1 μg/mL), with or without pre-incubation with the major constituents of selected EOs for 2 h. **LPS**: lipopolysaccharide; **Lin**: Linalool; **β-Cit**: β-Citronellol; **α-Thuj**: α-Thujone; **CPO**: Camphor; **Dexa**: Dexamethasone (50 μM). ** $p < 0.01$. Dexamethasone at 50 μM was used for comparison purposes.

caspase-1 inhibitory activity.

By showing the anti-inflammatory properties of EOs obtained from Tunisian flora, as well identifying the molecules responsible for said effect, we demonstrate the potential use of these samples as anti-inflammatory agents for both human and veterinary medicine.

CRediT authorship contribution statement

Renato B. Pereira: Conceptualization, Investigation, Data curation, Writing – original draft, Writing – review & editing. **Fatma Zohra Rahali:** Investigation, Writing – review & editing. **Ralph Nehme:** Writing – review & editing. **Hanen Falleh:** Writing – review & editing. **Mariem Ben Jemaa:** Investigation, Writing – review & editing. **Ibtissem Hamrouni Sellami:** Investigation, Writing – review & editing. **Riadh Ksouri:** Writing – review & editing. **Said Bouhallab:** Writing – review & editing. **Fabrizio Ceciliani:** Writing – review & editing. **Latifa Abdennebi-Najar:** Conceptualization, Resources, Writing – review & editing, Project administration, Funding acquisition. **David M. Pereira:** Conceptualization, Investigation, Data curation, Resources, Writing – original draft, Writing – review & editing.

Declaration of Competing Interest

The authors declare that they have no known competing financial interests or personal relationships that could have appeared to influence the work reported in this paper.

Data availability

Data will be made available on request.

Acknowledgements

Appendix A. Supplementary material

Supplementary data to this article can be found online at https://doi.org/10.1016/j.foodres.2023.112678.

References

Adams, R. (2005). Identification of essential oil components by gas chromatography/quadrupole mass spectroscopy. *Carol Stream, 16*, 65–120.

Bosshart, H., & Heinzelmann, M. (2016). THP-1 cells as a model for human monocytes. *Annals of Translational Medicine, 4*, 438. https://doi.org/10.21037/atm.2016.08.53

Boukamp, P., Petrussevska, R. T., Breitkreutz, D., Hornung, J., Markham, A., & Fusenig, N. E. (1988). Normal keratinization in a spontaneously immortalized aneuploid human keratinocyte cell line. *The Journal of Cell Biology, 106*, 761–771. https://doi.org/10.1083/jcb.106.3.761

Chen, L., Deng, H., Cui, H., Fang, J., Zuo, Z., Deng, J., … Zhao, L. (2018). Inflammatory responses and inflammation-associated diseases in organs. *Oncotarget, 9*, 7204–7218. https://doi.org/10.18632/oncotarget.23208

Chen, P. X., Bai, Q., Wu, Y. T., Zeng, Q. Z., Song, X. W., Guo, Y. Y., … Wang, Y. F. (2021). The essential oil of *Artemisia argyi* H.Lév. and vaniot attenuates NLRP3 inflammasome activation in THP-1 cells. *Frontiers in Pharmacology, 12*, Article 712907. https://doi.org/10.3389/fphar.2021.712907

De Groot, A. C., & Schmidt, E. (2016). Essential oils, part IV: Contact allergy. *Dermatitis, 27*, 170–175. https://doi.org/10.1097/DER.0000000000000197

Ehrnhöfer-Ressler, M. M., Fricke, K., Pignitter, M., Walker, J. M., Walker, J., Rychlik, M., & Somoza, V. (2013). Identification of 1,8-cineole, borneol, camphor, and thujone as anti-inflammatory compounds in a *Salvia officinalis* L. infusion using human gingival fibroblasts. *Journal of Agricultural and Food Chemistry, 61*, 3451–3459. https://doi.org/10.1021/jf305472t

Falleh, H., Ben Jemaa, M., Saada, M., & Ksouri, R. (2020). Essential oils: A promising eco-friendly food preservative. *Food Chemistry, 330*, Article 127268. https://doi.org/10.1016/j.foodchem.2020.127268

Furman, D., Campisi, J., Verdin, E., Carrera-Bastos, P., Targ, S., Franceschi, C., … Slavich, G. M. (2019). Chronic inflammation in the etiology of disease across the life span. *Nature Medicine, 25*, 1822–1832. https://doi.org/10.1038/s41591-019-0675-0

Gunaseelan, S., Balupillai, A., Govindasamy, K., Muthusamy, G., Ramasamy, K., Shanmugam, M., & Prasad, R. N. (2016). The preventive effect of linalool on acute and chronic UVB-mediated skin carcinogenesis in Swiss albino mice. *Photochemical & Photobiological Sciences, 15*, 851–860. https://doi.org/10.1039/c6 pp00075d

Huang, Y., Xu, W., & Zhou, R. (2021). NLRP3 inflammasome activation and cell death. *Cellular & Molecular Immunology, 18*, 2114–2127. https://doi.org/10.1038/s41423-021-00740-6

Ho, C. L., Li, L. H., Weng, Y. C., Hua, K. F., & Ju, T. C. (2020). Eucalyptus essential oils inhibit the lipopolysaccharide-induced inflammatory response in RAW264.7 macrophages through reducing MAPK and NF-κB pathways. *BMC Complementary Medicine and Therapies, 20*, 200. https://doi.org/10.1186/s12906-020-02999-0

Huo, M., Cui, X., Xue, J., Chi, G., Gao, R., Deng, X., … Wang, D. (2013). Anti-inflammatory effects of linalool in RAW 264.7 macrophages and lipopolysaccharide-induced lung injury model. *Journal of Surgical Research, 180*, e47–e54. https://doi.org/10.1016/j.jss.2012.10.050

Jayaganesh, R., Pugalendhi, P., & Murali, R. (2020). Effect of citronellol on NF-kB inflammatory signaling molecules in chemical carcinogen-induced mammary cancer in the rat model. *Journal of Biochemical and Molecular Toxicology, 34*, e22441.

Kim, M. H., Park, S. J., & Yang, W. M. (2020). Inhalation of essential oil from *Mentha piperita* ameliorates PM10-exposed asthma by targeting IL-6/JAK2/STAT3 pathway based on a network pharmacological analysis. *Pharmaceuticals, 14*, 2. https://doi.org/10.3390/ph14010002

Li, Y., Lv, O., Zhou, F., Li, Q., Wu, Z., & Zheng, Y. (2015). Linalool inhibits LPS-induced inflammation in BV2 microglia cells by activating Nrf2. *Neurochemical Research, 40*, 1520–1525. https://doi.org/10.1007/s11064-015-1629-7

Liao, J. M., Xie, X. Y., Wang, W. L., Gao, Y., Cai, Y. L., Peng, J. C., … Wang, L. (2021). Anti-inflammatory activity of essential oil from leaves of *Blumea balsamifera* (L.) DC through inhibiting TLR4/NF-kB signaling pathways and NLRP3 inflammasome activation in LPS-induced RAW264.7 macrophage cells. *Journal of Essential Oil Bearing Plants, 24*, 160–176. https://doi.org/10.1080/0972060X.2021.1912645

Liu, T., Zhang, L., Joo, D., & Sun, S.-C. (2017). NF-κB signaling in inflammation. *Signal Transduction and Targeted Therapy, 2*, 17023. https://doi.org/10.1038/sigtrans.2017.23

Miguel, M. G. (2010a). Antioxidant activity of medicinal and aromatic plants A review. *Flavour and Fragrance Journal, 25*, 291–312. https://doi.org/10.1002/ffj.1961

Miguel, M. G. (2010b). Antioxidant and anti-Inflammatory activities of essential oils: A short review. *Molecules, 15*, 9252–9287. https://doi.org/10.3390/molecules15129252

Mohamed, M. E., Abduldaium, Y. S., & Younis, N. S. (2020). Ameliorative effect of linalool in cisplatin-induced nephrotoxicity: The role of HMGB1/TLR4/NF-κB and Nrf2/HO1 pathways. *Biomolecules, 10*, 1488. https://doi.org/10.3390/biom10111488

Nehme, R., Andrés, S., Pereira, R. B., Ben Jemaa, M., Bouhallab, S., Ceciliani, F., … Abdennebi-Najar, L. (2021). Essential oils in livestock: From health to food quality. *Antioxidants, 10*, 330. https://doi.org/10.3390/antiox10020330

O'Brien, M., Moehring, D., Muñoz-Planillo, R., Núñez, G., Callaway, J., Ting, J., … Lazar, D. (2017). A bioluminescent caspase-1 activity assay rapidly monitors inflammasome activation in cells. *Journal of Immunological Methods, 447*, 1–13. https://doi.org/10.1016/j.jim.2017.03.004

Park, M. H., & Hong, J. T. (2016). Roles of NF-κB in cancer and inflammatory diseases and their therapeutic approaches. *Cells, 5*, 15. https://doi.org/10.3390/cells5020015

Pech-Puch, D., Joseph-Nathan, P., Burgueño-Tapia, E., González-Salas, C., Martínez-Matamoros, D., Pereira, D. M., … Rodríguez, J. (2021). Absolute configuration by vibrational circular dichroism of anti-inflammatory macrolide briarane diterpenoids from the Gorgonian *Briareum asbestinum*. *Scientific Reports, 11*, 496. https://doi.org/10.1038/s41598-020-79774-1

Pereira, R. B., Pereira, D. M., Jiménez, C., Rodríguez, J., Nieto, R. M., Videira, R. A., … Valentão, P. (2019). Anti-inflammatory effects of 5α,8α-Epidioxycholest-6-en-3β-ol, a steroidal endoperoxide isolated from *Aplysia depilans*, based on bioguided fractionation and NMR analysis. *Marine Drugs, 17*, 330. https://doi.org/10.3390/md17060330

Pérez, G. S., Zavala, S. M., Arias, G. L., & Ramos, L. M. (2011). Anti-inflammatory activity of some essential oils. *Journal of Essential Oil Research, 23*, 38–44. https://doi.org/10.1080/10412905.2011.9700480

Santos, P. L., Rabelo, T. K., Matos, J. P. S. C. F., Anjos, K. S., Melo, M. A. O., Carvalho, Y. M. B. G., … Quintans-Júnior, L. J. (2021). Involvement of nuclear factor κB and descending pain pathways in the anti-hyperalgesic effect of β-citronellol, a food ingredient, complexed in β-cyclodextrin in a model of complex regional pain syndrome - Type 1. *Food and Chemical Toxicology, 153*, Article 112260. https://doi.org/10.1016/j.fct.2021.112260

Sindle, A., & Martin, K. (2021). Art of prevention: Essential oils - natural products not necessarily safe. *International Journal of Women's Dermatology, 7*, 304–308. https://doi.org/10.1016/j.ijwd.2020.10.013

Spisni, E., Petrocelli, G., Imbesi, V., Spigarelli, R., Azzinnari, D., Donati Sarti, M., … Valerii, M. C. (2020). Antioxidant, anti-inflammatory, and microbial-modulating activities of essential oils: Implications in colonic pathophysiology. *International Journal of Molecular Sciences, 21*, 4152. https://doi.org/10.3390/ijms21114152

Su, Y. W., Chao, S. H., Lee, M. H., Ou, T. Y., & Tsai, Y. C. (2010). Inhibitory effects of citronellol and geraniol on nitric oxide and prostaglandin E_2 production in macrophages. *Planta Medica, 76*, 1666–1671. https://doi.org/10.1055/s-0030-1249947

Tran, T. A. T., Grievink, H. W., Lipinska, K., Kluft, C., Burggraaf, J., Moerland, M., … Malone, K. E. (2019). Whole blood assay as a model for *in vitro* evaluation of inflammasome activation and subsequent caspase-mediated interleukin-1 beta release. *PLoS One, 14*, e0214999.

Vonkeman, H. E., & van de Laar, M. A. (2010). Nonsteroidal anti-inflammatory drugs: Adverse effects and their prevention. *Seminars in Arthritis and Rheumatism, 39*, 294–312. https://doi.org/10.1016/j.semarthrit.2008.08.001

Yoon, W. J., Moon, J. Y., Song, G., Lee, Y. K., Han, M. S., Lee, J. S., … Hyun, C. G. (2010). *Artemisia fukudo* essential oil attenuates LPS-induced inflammation by suppressing NF-kappaB and MAPK activation in RAW 264.7 macrophages. *Food and Chemical Toxicology, 48*, 1222–1229. https://doi.org/10.1016/j.fct.2010.02.014

Zhou, J. Y., Tang, F. D., Mao, G. G., & Bian, R. L. (2004). Effect of alpha-pinene on nuclear translocation of NF-kappa B in THP-1 cells. *Acta Pharmacologica Sinica, 25*, 480–484.